JOINT EUROPEAN TORUS

JET–P(92)30

B. Wolle, L-G Eriksson
and JET Team

Time-dependent Neutron Rate Interpretation for Neutral Beam Heated Tokamaks

Time-dependent Neutron Rate Interpretation for Neutral Beam Heated Tokamaks

B. Wolle, L-G Eriksson
and JET Team*

JET-Joint Undertaking, Culham Science Centre, OX14 3DB, Abingdon, UK

[1]*Institute for Applied Physics, Heidelberg University, Heidelberg, FRG*
** See Annex*

Preprint of Paper to be submitted for publication in
Plasma Physics and Controlled Fusion

Time-dependent Neutron Rate Interpretation for Neutral Beam Heated Tokamaks

B. WOLLE*, L.-G. ERIKSSON
JET Joint Undertaking, Abingdon, Oxon. OX14 3EA, UK.
* Institute for Applied Physics, Heidelberg University, D-6900 Heidelberg, F.R.G.

ABSTRACT

Neutron diagnostics offer one of the most direct ways to obtain information about the deuteron characteristics in fusion plasmas such as densities and temperatures. Thus, neutron diagnostics are of increasing importance for future fusion devices and efforts are being made to improve the present methods for interpreting neutron signals. Until now, however, the derivation of deuteron densities as functions of time for non-stationary neutral beam heated plasmas, i.e. where the velocity distribution of the plasma deuterons is highly non-Maxwellian and steady-state conditions have not been reached, was only possible in very few cases with the aid of slow, complex codes. Here, we present a comparatively fast, time-dependent code for neutron rate interpretation of neutral beam heated tokamak plasmas which is based on a Fokker-Planck model for injected ions. The code includes tail-tail fusion reaction rates, which are important but often had to be neglected since they are difficult to calculate. Results from the code are presented for test cases in order to illustrate the time-scales involved in neutron production. Finally, time-dependent interpretation calculations for JET hot-ion mode discharges are presented, and the results for the inferred dilution n_D/n_e are shown to be in very good agreement with the experimental data.

1. INTRODUCTION

Neutral beam injection (NBI) has become a widely used method for auxiliary heating of tokamak plasmas. In large tokamaks such as JET, TFTR and JT-60 it is one of the main supplementary heating methods with the potential of injecting more than 20 MW of fast neutral atoms into the plasma (DUESING *et al.*, 1987; GRISHAM *et al.*, 1985; MATSUDA *et al.*, 1987), as compared to 1-3 MW ohmic power. As a consequence of the injection, the velocity distribution of the injected ions becomes non-Maxwellian, leading to a strong enhancement of the fusion reaction rate above the thermal level. Using the measured fusion reaction rate, e.g. measured neutron rates, it is possible to carry out interpretation calculations by modelling of the ion velocity distribution and extract plasma parameters

such as densities and temperatures. For Maxwellian plasmas this is a straightforward procedure and recent works report good agreement with results of other diagnostics (JARVIS *et al.*, 1987; 1989). To treat neutral beam heated plasmas, it is important to use models which describe the non-Maxwellian velocity distributions with sufficient accuracy. Sophisticated but time-consuming codes, such as TRANSP (HAWRYLUK, 1980; GOLDSTON *et. al.*, 1981), are used to obtain information about the plasma deuterons. These codes attempt to obtain concistency between all measured plasma parameters within small variations of their values. However, the computing time needed to evaluate the ion velocity distribution has to be kept sufficiently short in order to make these calculations practicable for routine analysis, i.e. for more than a very small sample of experimental conditions. To achieve this, a simple relaxation-time model, whose application is restricted to low temperatures, has been used successfully by HÜBNER *et al.*, (1985), (1988). Others (STRACHAN *et al.*, 1981; HENDEL *et al.*, 1986) used a more sophisticated but also more time-consuming time-dependent Fokker-Planck model. However, they reported discrepancies of up to a factor 2-3 between calculations and measurements in some cases. Then, in a work by WOLLE *et al.* (1991), using a fast steady-state Fokker-Planck model, parameter ranges for interpretation calculations in relation to the errors in the measured input data could be identified. The results of interpretation calculations were shown to be in good agreement with measurements and, in particular, the errors of the evaluated dilution ratios were smaller than those from other diagnostics.

In this paper we present the first results from a code for time-dependent interpretation of neutron rate measurements. As an application, a number of JET hot ion mode discharges are analysed. They show that the time evolution of the inferred dilution ratio n_D/n_e is in good agreement with other independent measurements.
Furthermore, we illustrate how the different time-scales involved in the evolution of the deuterium velocity distribution, i.e the ion-ion and the ion-electron collisional time scales, affect the fusion neutron production.

It is important to include the time-dependence, especially when the background parameters or the injection power vary on a time scale shorter than, or comparable with the ion-electron slowing-down time. This is often the case in JET and other large tokamaks. For these plasmas, a stationary model can substantially overestimate the neutron rate and can, therefore, lead to discrepancies between the inferred deuteron parameters and the measurements. The time-dependence is the main advantage of the present code as compared to the one in WOLLE *et al.*, (1991) since this extends the range of application to dynamic plasmas or the early phase of the injection.

The code is based on the time-dependent Fokker-Planck equation including relevant source and loss terms. In order to make the computation time sufficiently short for routine analysis, the 2D Fokker-Planck equation is solved by expanding the distribution in the eigenfunctions of the pitch angle scattering operator. Thus the problem is reduced to a set of 1D parabolic differential equations.

Usually, only the first few orders (typically 4-6) need to be calculated to obtain a reasonable accuracy. The computing time is therefore fairly short.

We solve the 1D equations with a finite element method since it is flexible and the boundary conditions are easily implemented. Furthermore, there are no problems with using a non-uniform grid, which is essential for treating NBI where the source is rather narrow. The method of solution and the calculation of velocity moments using finite elements is briefly outlined.

2. INTERPRETATION CODE

The code presented here, called NR-FPS (Neutron-Rate Fokker-Planck Solver), has a fully modular structure. A software module which is easily adapted to changes in central data banks or to newly available diagnostics data reads all the input data. These input data are, exept for the neutral beam depostition profile, all measured. The latter has to be calculated through deposition codes which are using the measured data as well.
The local time-dependent distribution functions and the corresponding reactivities are calculated in the main module. The value of the plasma parameters of interest, for example n_D, is then obtained using an iteration technique. There, the evolution of the distribution function from the previous time-point is calculated by varying the plasma parameter of interest in such a way that the measured and calculated neutron rates agree. This agreement is after 3-4 iterations typically better than 1%. It should be noted that the output of an interpretation calculation comprises, apart form the iterated value of the plasma parameter, the composition of the measured neutron rate with respect to thermal, beam-thermal and beam-beam components of origin.

Of course, our code not only allows the determination of plasma parameters through neutron rate interpretation as mentioned above, but also prediction of neutron rates and neutron emission profiles. As we have shown in WOLLE and ERIKSSON (1992), the agreement between prediction and measurement can on average be better than 20%, provided the input data are measured with sufficient accuracy. This compares to a report by CORRIGAN *et al.* (1992) where an overall accuracy of approximately 40% for neutron rate calculations from TRANSP or PENCIL (STUBBERFIELD *et al.*, 1987) was found. This is, however, not surprising since TRANSP is using the less accurate cross-section data from DUANE (1972) and furthermore usually only 1000 Monte-Carlo particles are followed in the Fokker-Planck calculation in order to represent the velocity distribution in 20 spacial sections in the plasma. On the other hand, in the PENCIL code which uses the more accurate cross-section data from PERES (1979), the tail-tail reaction rate is neglected.

3. FOKKER-PLANCK EQUATION

The equation which determes the evolution of the 2D velocity distribution $f(v,\mu,t)$ for the injected ions in the presence of neutral beam injection is the Fokker-Planck equation

$$\frac{\partial U(v,\mu,t)}{\partial t} = \frac{\partial}{\partial v}\left\{-\alpha U + \frac{1}{2}\frac{\partial}{\partial v}(\beta U)\right\} + \frac{\gamma}{4v^2}\frac{\partial}{\partial \mu}\left[(1-\mu^2)\frac{\partial U}{\partial \mu}\right] + S(v,\mu) - L(v). \qquad (1)$$

where $U(v,\mu,t) = v^2 f(v,\mu,t)$, $\mu = v/v_{\|}$ is the pitch angle variable, S is a source term, L is a loss term and the collision coefficients (see for instance STIX, 1975) are given by:

$$\alpha = \langle \Delta v_{\|} \rangle + \frac{1}{2v}\langle (\Delta v_{\perp})^2 \rangle, \qquad \beta = \langle (\Delta v_{\|})^2 \rangle, \qquad \gamma = \langle (\Delta v_{\perp})^2 \rangle. \qquad (2)$$

Different models can be used for the loss term. Most common are charge exchange models or models taking into account both finite particle and energy confinement (KILLEEN *et al.*, 1986). Sometimes, a simple Gaussian loss term as reported by ANDERSON *et al.* (1981) can also be used.

By expanding $U(v,\mu,t)$ in Legendre polynomials P_n, which are eigenfunctions of the pitch-angle scattering term, as:

$$U(v,\mu,t) = \sum_{i=1}^{\infty} a_n(v,t)\, P_n(\mu), \qquad (3)$$

the two-dimensional Fokker-Planck equation can be written as an infinite set of one-dimensional equations for $a_n(v,t)$ of each order n. The resulting 1D partial differential equation for each n is:

$$\frac{\partial a_n(v,t)}{\partial t} = \frac{\partial}{\partial v}\left\{-\alpha a_n + \frac{1}{2}\frac{\partial}{\partial v}(\beta a_n)\right\} - \frac{\gamma}{4v^2} n(n+1) a_n + k_n S(v) - \frac{1}{\tau_c} a_n \qquad (4)$$

with the boundary conditions

$$\lim_{v\to\infty} a_n = 0 \quad \text{and} \quad \begin{cases} 4\pi \int_0^{\infty} a_n v^2 dv = n_D, \quad \left.\frac{da_n}{dv}\right|_{v=0} = 0 & \text{for } n = 0, \\ \lim\limits_{v\to 0} a_n = 0 & \text{for } n > 0. \end{cases} \qquad (5)$$

Furthermore, k_n are coefficient functions for the expansion of the angular spread of the injection in Legendre polynomials and τ_c is the particle confinement time. Eq. (4) now can be solved with our numerical scheme. It should be mentioned here that the zeroth order solution $a_0(v,t)$ is just the pitch-angle averaged distribution function.

Introducing the following coefficient functions $A(x)$, $B(x)$, $C(x)$ and $D(x)$:

$$A = -\alpha + \frac{1}{2}\frac{\partial B}{\partial x}, \quad B = \frac{1}{2}\beta, \quad C = -\frac{\gamma}{4x^2}n(n+1) - \frac{1}{\tau_c}, \quad D = k_n S(x), \tag{6}$$

we can rewrite Eq. (4) more generally as a parameterised parabolic differential equation of a function $U(x,t)$, where $U = a_n$ and $x = v$:

$$\frac{\partial U}{\partial t} = \frac{\partial}{\partial x}\left\{A(x)U + B(x)\frac{\partial U}{\partial x}\right\} + C(x)U + D(x). \tag{7}$$

The method of solving Eq. (7) with finite elements is outlined in Appendix A.

4. VELOCITY SPACE MOMENTS

For our application, it is necessary to calculate the fusion reactivity which, for a plasma containing ion species of type (a) and (b), is given by:

$$\langle \sigma v \rangle = 8\pi^2 \sum_{n=0}^{\infty} \frac{1}{2n+1} \int_0^{\infty} a_n(v) \int_0^{\infty} b_n(v') \int_{-1}^{1} P_n(\mu)\, \sigma(u)\, u \; d\mu \, dv' dv \tag{8}$$

as shown by CORDEY *et al.* (1978), where a_n and b_n are the n^{th} order coefficient functions from the expansion of the ion distributions in Legendre polynomials P_n and $u^2 = v^2 + v'^2 - 2vv'\mu$. For the cross-section σ, new available fit data by BOSCH and HALE (1990) have been used here, since this data provides a higher degree of accuracy than the cross-section data from DUANE (1972) or PERES (1979) which are commonly used in other codes.

Many other important moments, which are used for diagnostic purpose in our code, can be expressed as linear moments of the velocity distribution in the following form:

$$\langle g(v) \rangle = \int_0^{\infty} g(v) U(v,t)\, dv. \tag{9}$$

The lowest order moment for instance is the density for $g(v) = 1$, the second order moment is the energy content for $g(v) = {}^1/_2 mv^2$ and so on.

The equivalent expressions for the above given equations (8) and (9) with the linear finite elements used in our code are given in Appendix B.

5. NUMERICAL RESULTS

We considered a plasma with $T_e = T_i = 5$ keV, $n_e = n_D = 2 \cdot 10^{13}\text{cm}^{-3}$ and 80 keV D^0-injection with a source rate of $S_0 = 2 \cdot 10^{13}\text{cm}^{-3}\text{s}^{-1}$. In order to resolve the source term numerically, the delta-function was replaced by a Gaussian. The injection angle was set to 45° and source and loss term have been balanced. The calculated distribution function is plotted in Fig. 1 as a function of time. The power transferred due to collisions is shown in Fig. 2, the total fusion reactivities for the pitch-angle averaged distribution function and the anisotropic case are given in Fig. 3 as a function of time for the DD neutron branch.

In this example, the slowing-down time for the ions on electrons is $\tau_s \approx 1.25$ s. Spitzer's critical energy E_α, below which collisions on ions are more important than collisions on electrons, is:

$$E_\alpha = 14.8\, T_e \left[\frac{A^{3/2}}{n_e} \sum_j \frac{n_j Z_j^2}{A_j} \right]^{2/3} \tag{10}$$

where A and A_j are the atomic masses of the test and j species of field ions, n_e is in cm^{-3} and T_e in eV. The critical energy in our test case is about 93 keV. The time it takes to establish the velocity distribution below the injection velocity t_{st}, i.e. the time it takes for a particle to slow down from the injection velocity to the thermal region, can be estimated from the time-dependent Fokker-Planck equation. Using the high energy approximation neglecting diffusive terms, we obtain:

$$t_{st} = \frac{\tau_s}{3} \ln\left(1 + \left(\frac{E_o}{E_\alpha} \right)^{3/2} \right) \tag{11}$$

where E_0 is the injection energy. With the values given above, $t_{st} \approx 0.25$ s and more than 90% of the steady-state reaction rate is reached after this time, while after $2t_{st}$ steady-state conditions have been reached. In Fig. 4, the neutron rates due to thermal, beam-thermal and beam-beam neutron production are plotted vs. time. It should be pointed out here that we define the "thermal" part of the actual particle distribution by an asymptotic and isotropic Maxwellian at low velocities and thus artificially splitting the unique particle distribution into two parts, i.e. "thermal" and "beam" part. In this sense, the neutron rate and the reactivities can be split into thermal, beam-thermal and beam-beam components. Since the beam-thermal neutron production is mostly affected by slowing-down processes, the steady-state level is almost reached by a time of t_{st}. For the beam-beam neutron production however, the much slower diffusive time scale is relevant and thus quasi steady-state conditions are reached much later in this example.

The expression for t_{st}, eq. (11), gives a criterion for when steady-state calculations are valid. In order to resolve the evolution of the neutron rate on time scales shorter than the one given by t_{st}, time-dependent calculations are necessary.

6. NEUTRON RATE INTERPRETATION CALCULATIONS

To demonstrate the applicability of our method for complicated problems, we present calculations for the JET hot-ion H-mode discharges #18757, #18768 and #18589 which have been discussed in some detail before (ADAMS *et al.*, 1990; BALET *et al.*, 1990; WATKINS *et al.*, 1989). These discharges are part of a series of experiments performed to optimise the fusion reactivity in JET using intense 80 keV neutral beam injection. To achieve high fusion reactivities, the injected deuterons have to slow down mainly on ions in order to heat them. This implies high electron temperatures and low electron densities. Due to the low electron density, the neutron rate is very sensitive to small changes of the deuteron density and thus interpretation calculations to determine n_D/n_e-ratios can be carried out with good accuracy (WOLLE *et al.*, 1991). The discharges presented here cover some range in input power, density and neutron rate and show a quite different time behaviour for the neutron rate as shown in Fig. 5.
The input plasma data to our calculations comprise the measured electron temperature profiles from ECE, the electron density profiles from the FIR interferometer, the previously calculated deposition profiles from PENCIL (STUBBERFIELD *et al.*, 1987) and the measured ion temperature profiles from the charge exchange recombination spectroscopy CXRS (BOILEAU *et al.*, 1989). We furthermore assume carbon as inpurity ion species with a flat Z_{eff} profile. Analysing discharges, we follow the deuteron velocity distribution in time for 11 flux surfaces and iteratively calculate the dilution ratio n_D/n_e from the measured neutron rates for typically 10-20 time points of interest during the neutral beam injection phase. These time points have been chosen according to the availability of measured experimental data. In the cases presented here, the calculated neutron rates using the obtained dilution ratio after 3 iterations is matching the measured neutron rates rather accurately. For the above given pulses, this is shown in Figs. 6-8 where the total neutron rate and its calculated composition with respect to thermal, beam-thermal and beam-beam production is plotted in time together with the measurements.

Due to the low density at the beginning of the injection phase for the discharges #18757 and #18768, the slowing-down time scale is relatively long, which leads to a comparatively large fraction of fast ions, typically more than 40% of the density of the injected species. Thus the non-thermal neutron production and in particular the beam-beam neutron production dominates. The starting density of pulse #18589 is about a factor of 2 larger than in the other two discharges, which leads to shorter slowing-down times and thus a smaller fraction of fast ions. The beam-beam neutron rate is therefore not as dominating. Instead, the beam-thermal and the total neutron rates are increasing on a faster time scale. For slightly later times in the two very low density pulses, with increasing thermal density, the beam-thermal neutron production starts to contribute significantly to the total neutron production, while the beam-beam production however still remains dominating. For the time between 0.8 and 2.0 seconds for

the pulse #18757, 0.6 - 1.0 seconds for #18768 and 0.4 - 1.1 seconds for discharge #18589 after switching on the neutral beam, the deuteron density remains approximately constant while the electron density is still rising. This leads to shorter slowing-down times and therefore to a decrease of the fast particle density to values of 20-40% of the deuteron density. The beam-beam neutron production is therefore decreasing and most of the neutrons originate from beam-thermal production, in these cases between 60 and 70%. Fig. 9 shows the contributions of the beam-beam, beam-thermal and thermal-thermal neutron rates for the three pulses at different time points as a function of the averaged deuteron density $\langle n_D \rangle$. Our analysis shows that for the highest neutron rates, the beam-thermal fraction is $\approx$ 60%, the beam-beam part is $\geq$ 25% and the averaged deuteron density is $0.7\text{-}1.1 \cdot 10^{19} m^{-3}$.
Finally, Figs. 10-12 show the obtained n_D/n_e-values for the different discharges as a function of time together with the measured data from the CXRS-diagnostics and the values obtained from the visible bremsstrahlung Z_{eff} assuming carbon as impurity ion species. Clearly, the different n_D/n_e-traces agree well which demonstrates the potential of our methods for future plasma diagnostics. However, the calculated dilution for the time point at 10.0 seconds in pulse #18589 differs quite from the results of the measurements. A possible reason for this might be the application of low power ICRH heating. The ICRH power was linearly rising from 9.5 seconds to 10.25 seconds reaching 1.45 MW. During the 20 MW neutral beam injection phase, effects of 1.45 MW ICRH are rather small and can thus be neglected. For the low temperatures in the pre-beam-phase of the discharge, a small distortion of the deuteron distribution can have a noticeable effect on the fusion reaction rate. Further calculations with our code show that a distortion of the deuteron distribution which corresponds to 0.1 MW NBI heating at 80 keV would reduce the obtained dilution ratio to the measured value.

With the plasma data of the pulse #18757, the 2D-distribution was calculated using the first 5 eigenfunctions for 21 time points with 11 points radial resolution. For each eigenvalue, time and radius point, the fusion reactivity was calculated. The computation time for this problem involving 1155 Fokker-Planck solutions and reactivity calculations was 181 seconds on the IBM 3090. As shown in table 1, most of the time (about 86%) was spent to solve the Fokker-Planck equation.

7. CONCLUSIONS

Our fast neutron rate interpretation code allows the determination of plasma parameters, e.g. deuteron densities, as a function of time from neutron rate measurents for neutral beam heated tokamak plasmas. The code is suitable for routine analysis and calculates most of the important velocity space moments. In the calculations of the neutron rate, the 2D character, i.e. anisotropy, of the velocity distribution is fully taken into account. For a single time and radius point, the calculation of the deuteron distribution and the reactivity calculation takes approximately 0.15 s CPU time on the IBM 3090.

A set of calculations for a test case has been used to discuss the time scales for the evolution of the deuteron velocity distribution and the neutron production in the precence of neutral beam injection.
An approximate expression to estimate the time it takes to establish the velocity distribution was given. These estimated times were found to be in good agreement with the numerical results. Thus, the approximate expression is useful to determine for which cases it is absolutely necessary to perform time-dependent calculations.

As a major achievement of this work, a detailed time-dependent neutron interpretation analysis for JET hot-ion mode discharges has been carried out where, for the first time, n_D/n_e-ratios have been calculated directly as functions of time from the measured neutron rates.
The results of our interpretation calculation agree well with the data of other diagnostics.
Our analysis furthermore shows that for the highest neutron rates in the discharges considered here, the beam-thermal fraction is about 60% and the beam-beam part is above 25%. For the early stage in the injection phase, most of the neutrons originate from tail-tail reactions.

Calclulations for low power ICRH heating in one of the cases discussed here, shows that the inferred dilution ratios significantly deviate from the measurements. This seems to indicate a distortion of the deuteron distribution, probably caused by 2^{nd} harmonic heating. Thus, for future work, modelling of ICRH should be included in the interpretation calculations.

APPENDIX A.

There are different standard computational techniques to solve the following parabolic differential equation:

$$\frac{\partial U}{\partial t} = \frac{\partial}{\partial x}\left\{A(x)U + B(x)\frac{\partial U}{\partial x}\right\} + C(x)U + D(x). \tag{A1}$$

When using finite elements to solve Eq. (A1), the first step is to express it in a variational form. Since a functional does not exist for this equation, the Ritz method to find an approximate solution to variational problems can not be applied in this case. The Galerkin method, however, provides an approximate solution to differential equations directly whether a functional exists or not. In the Galerkin finite element method, the approximate solution is written in terms of nodal unknowns as:

$$U(x,t) = \sum_{j=1}^{N} U_j(t)\,\Phi_j(x) \tag{A2}$$

where $U_j(t)$ are unknown coefficients and $\Phi_j(x)$ are finite elements. This equation can be interpreted as an interpolation of the local point solutions U_j. The finite elements are usually chosen from low-order piecewise polynomials restricted to contiguous elements. Linear one-dimensional finite elements are for instance shown in Fig. 13.
By rewriting Eq. (A1) in a variational form according to the Galerkin method its solution is approximated by a system of N ordinary differential equations for the N unknowns $U_1(t),\ldots, U_N(t)$. In vector notation it can be written as:

$$M_{kj}U_j' + (K_{kj} + L_{kj})\,U_j - V_k = 0 \tag{A3}$$

where prime denotes the time derivative and M, K, L and V are given by:

$$M_{kj} = \int_{x_1}^{x_N} \Phi_k \Phi_j \, dx, \qquad K_{kj} = \int_{x_1}^{x_N} \frac{\partial \Phi_k}{\partial x}\left\{A\Phi_j + B\frac{\partial \Phi_j}{\partial x}\right\} dx,$$

$$L_{kj} = \int_{x_1}^{x_N} C\,\Phi_k \Phi_j \, dx, \qquad V_k = \int_{x_1}^{x_N} D\,\Phi_k \, dx. \tag{A4}$$

Using a Cranck-Nicholson scheme for the time discretisation, Eq. (A3) is approximated by the following system of algebraic equations:

$$\left[M_{kj} + \tfrac{1}{2}\Delta t\,(K_{kj} + L_{kj})\right] U_j^{h+1} = \left[M_{kj} - \tfrac{1}{2}\Delta t\,(K_{kj} + L_{kj})\right] U_j^{h} + \Delta t\, V_k \tag{A5}$$

where U_j^h denotes U_j at $t = t_h$ and $\Delta t = t_{h+1} - t_h$. With linear finite elements, one obtains tridiagonal matrices for M, K, L and a vector for V, as given in WOLLE and ERIKSSON (1992). Thus Eq. (A5) can be solved easily with standard methods.

APPENDIX B.

Linear moments, $\langle g(v) \rangle$, of the velocity distribution $U(v,t)$ can be expressed in finite elements Φ_j as:

$$\langle g(v) \rangle = \int_{v_1}^{v_N} \sum_{ij} g_j(v_j)\, \Phi_j\, U_i(v_i)\, \Phi_i\, dv = \sum_{ij} U_i(v_i)\, g_j(v_j) \int_{v_1}^{v_N} \Phi_i\, \Phi_j\, dv$$

$$= \sum_i U_i(v_i) \{ g(v_{i-1})\, T_{i,i-1} + g(v_i)\, T_{i,i} + g(v_{i+1})\, T_{i,i+1} \} \qquad \text{(B1)}$$

with

$$T_{i,i-1} = \tfrac{1}{6}(v_i - v_{i-1}),$$

$$T_{i,i} = \tfrac{1}{3}(v_{i+1} - v_{i-1}),$$

$$T_{i,i+1} = \tfrac{1}{6}(v_{i+1} - v_i) \qquad \text{(B2)}$$

for linear finite elements.

To express the fusion reactivity, Eq. (8), in finite elements, we introduce:

$$a_n(v) = \sum_i {}^a U_i(v_i)\, \Phi_i,$$

$$b_n(v') = \sum_j {}^b U_j(v_j')\, \Psi_j \qquad \text{(B3)}$$

and

$$g_n(v,v') = \int_{-1}^{1} P_n(\mu)\, \sigma(u)\, u\, d\mu = \sum_{k,l} {}^n C_{k,l}\, \Phi_k \Psi_l \qquad \text{(B4)}$$

with $g_n(v,v') = {}^n C_{k,l}$. Now, the fusion reactivity can be approximated with linear finite elements as:

$$\langle \sigma v \rangle = 8\pi^2 \sum_n \frac{1}{2n+1} \sum_{ij} {}^a U_i(v_i)\, {}^b U_j(v_j') \times$$

$$\Big({}^n C_{i-1,j-1}\, T_{i,i-1}\, T_{j,j-1} + {}^n C_{i-1,j}\, T_{i,i-1}\, T_{j,j} + {}^n C_{i-1,j+1}\, T_{i,i-1}\, T_{j,j+1} +$$

$$+ {}^n C_{i,j-1}\, T_{i,i}\, T_{j,j-1} + {}^n C_{i,j}\, T_{i,i}\, T_{j,j} + {}^n C_{i,j+1}\, T_{i,i}\, T_{j,j+1} +$$

$$+ {}^n C_{i+1,j-1}\, T_{i,i+1}\, T_{j,j-1} + {}^n C_{i+1,j}\, T_{i,i+1}\, T_{j,j} + {}^n C_{i+1,j+1}\, T_{i,i+1}\, T_{j,j+1} \Big). \qquad \text{(B5)}$$

Acknowledgements – The authors acknowledge the contribution of the JET team in the production of the data used in this paper. They are in particular grateful to Dr. M. VON HELLERMANN from the charge exchange diagnostic group and Dr. G. SADLER from the neutron diagnostic group. Furthermore, one of the authors, B. WOLLE, would like to thank JET Theory Division for its hospitality and Profs. D. DÜCHS and K. HÜBNER for their encouraging interest in this work.

References

ADAMS J. M., BALET B., BOYD D. A., CAMPBELL D. J., CHALLIS C. D., CHRISTIANSEN J. P., CORDEY J. G., CORE W. G. F., COSTLEY A. E., COTTRELL G. A., EDWARDS A. W., ELEVANT T., ERIKSSON L.-G., HELLSTEN T., JARVIS O. N., LALLIA P. P., LAWSON K., LOWRY C., NIELSEN P., SADLER G., START D. F. H., THOMAS P. R., VON HELLERMANN M. and WEISEN H. (1991), *Nucl. Fusion* **31**, 891.

ANDERSON D., CORE W., ERIKSSON L.-G., HAMNÉN H., HELLSTEN T., and LISAK M. (1988), *Physica Scripta* **37**, 83.

BALET B., BOYD D. A., CAMPBELL D. J., CHALLIS C. D., CHRISTIANSEN J. P., CORDEY J. G., CORE W. G. F., COSTLEY A. E., COTTRELL G. A., EDWARDS A. W., ELEVANT T., ERIKSSON L.-G., HELLSTEN T., JARVIS O. N., LALLIA P. P., LAWSON K., LOWRY C., MORGAN P. D., NIELSEN P., SADLER G., START D. F. H., THOMAS P. R., THOMSEN K., VON HELLERMANN M. and WEISEN H. (1990), *Nucl. Fusion* **30**, 2029.

BOILEAU A., VON HELLERMANN M., HORTON L. D., SPENCE J. and SUMMERS H. P. (1989), *Plasma Phys. Contr. Fusion* **31**, 779.

BOSCH H.-S., and HALE G. M. (1990), *Proc. 17th Eur. Conf. on Controlled Fusion and Plasma Heating*, Amsterdam, 1990, Vol. 14B, Part II, p. 873.

CORDEY J. G., MARX K. D., MCCOY M. G., MIRIN A. A. and RESNIK M. E. (1978), *J. Comput. Phys.* **28**, 115.

CORRIGAN G., MUIR D. G. and TIBONE F. (1992), Neutral Beam-Plasma Interaction in JET: Comparison of PENCIL and TRANSP Modelling Results, Rep. JET-R(91) 14, JET Joint Undertaking, Abingdon, Oxfordshire.

DUANE, B. H. (1972), *Annual Report on CTR Technology* 1972, Report BNWL-1685, Batelle Pacific Northwest Lab., Richland.

DUESING G., ALTMANN H., FALTER H., GOEDE A., HANGE R., HEMSWORTH R. S., KUPSCHUS P., STORK D. and THOMPSON E. (1987), *Fusion Technology* **11** (1), 163.

GOLDSTON R. J., MCCUNE D. C., TOWNER H. H., DAVIS S. L., HAWRYLUK R. J. and SCHMIDT G. L. (1981) *J. Comput. Phys.* **43**, 61.

GRISHAM L. R., EUBANK H. P., KAMPERSCHROER J. H., KUGEL H. W., MARTIN G. D., PRECHTER R. E., PRICHARD JR B. A., WILLIAMS M. D., WINJE R. A. and WRIGHT K. E. (1985), *Nucl. Instr. and Methods* **B10/11**, 478.

HAWRYLUK R. J. (1980) *Proc. International School of Plasma Physics, Course of Physics of Plasmas close to Thermonuclear Conditions*, Varenna, 1979, Vol. 1, p. 19.

HENDEL H. W., ENGLAND A. C., JASSBY D. L., MIRIN A. A. and NIESCHMIDT E. B. (1986) *J. Fusion Energy* **5**, 231.

HÜBNER K., BÄTZNER R., HINSCH H. *et al.*, (1985), *Proc. 12th Eur. Conf. on Controlled Fusion and Plasma Physics*, Budapest, 1985, Vol. 9F, Part I, p. 231.

HÜBNER K., BÄTZNER R., BOMBA B. *et al.*, (1988), *Proc. 15th Eur. Conf. on Controlled Fusion and Plasma Heating*, Dubrovnik, 1988, Vol. 12B, Part III, p. 1191.

JARVIS O. N., GORINI G., KÄLLNE J., MERLO V., SADLER G. and VAN BELLE P. (1987), *Nucl. Fusion* **27**, 1755.

JARVIS O. N., ADAMS J. M., BALET B., CONROY S., CORDEY J. G., ELEVANT T., GILL R. D., LOUGHLIN M. J., MANDL W., MORGAN P. D., PASINI D., SADLER G., WATKINS M., VAN BELLE P., VON HELLERMANN M. and WEISEN H. (1990), *Nucl. Fusion* **30**, 308.

KILLEEN J., KERBEL G. D., MCCOY M. G. and MIRIN A. A. (1986), Computational Methods for Kinetic Models of Magnetically Confined Plasmas, *Springer Ser. Comput Phys.* (Springer, New York, Berlin, Heidelberg, Tokyo).

MATSUDA S., AKIBA M., ARAKI M., DAIRAKU M., EBISAWA N., HORIIKE H., ITOH T., KANAI T., KAWAI M., KOMATA M., KURIYAMA M., KITAMURA S., MATSUOKA M., MIZUHASHI K., OHGA T., OHHARA H., OHUCHI Y., OHARA Y., OKUMURA Y., SHIBANUMA K., SHIBATA T., SHIRAKATA H., SUGAWARA T., TANAKA S. and WATANABE K. (1987) *Fusion Eng. and Design* **5**, 85.

PERES, A. (1979), *J. Appl. Phys.*, **50**, 5569.

STIX T. H. (1975), *Nucl. Fusion* 15, 737.

STRACHAN J. D., COLESTOCK P. L., DAVIS S. L., EAMES D., EFTHIMION P. C., EUBANK H. P., GOLDSTON R. J., GRISHAM L. R., HAWRYLUK R. J., HOSEA J. C., HOVEY J., JASSBY D. L., JOHNSON D. W., MIRIN A. A., SCHILLING G., STOCKSBERRY R., STEWART L. D. and TOWNER H. H. (1981) *Nucl. Fusion* **21**, 67.

STUBBERFIELD P. M. and WATKINS M. L. (1987), JET Experimental Department Research Note DPA(06)87, Multiple Pencil Beam.

WATKINS M. J., BALET B., BHATNAGAR V. P., CORDEY J. G., HAMMETT G. W. HELLSTEN T., KEILHACKER M., MILORA S. L., MORGAN P. D., SACK C., SCHMIDT G. L., TARONI A., THOMAS P. R., THOMSEN K., TIBONE F., VON HELLERMANN M. and WEISEN H. (1989), *Plasma Phys. and Contr. Fusion* **31**, 1713.

WOLLE B., ERIKSSON L.-G., HÜBNER K., MORGAN P. D., MORSI H. W., SADLER G. and VON HELLERMANN M. G. (1991), *Plasma Phys. and Contr. Fusion* **33**, 1863.

WOLLE B. and ERIKSSON L.-G. (1992), A Time-dependent Fokker-Planck Code for Neutron Rate Interpretations, Rep. JET-R(92)02, JET Joint Undertaking, Abingdon, Oxfordshire.

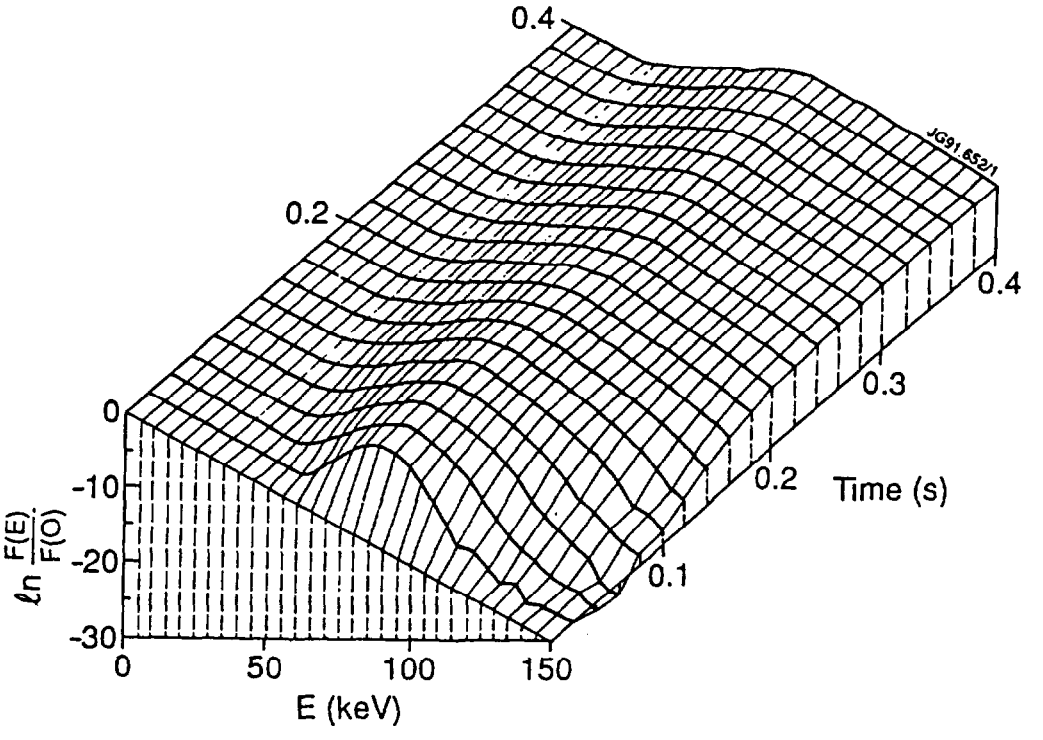

FIG. 1. — Evolution of the distribution function in time for the test case data.

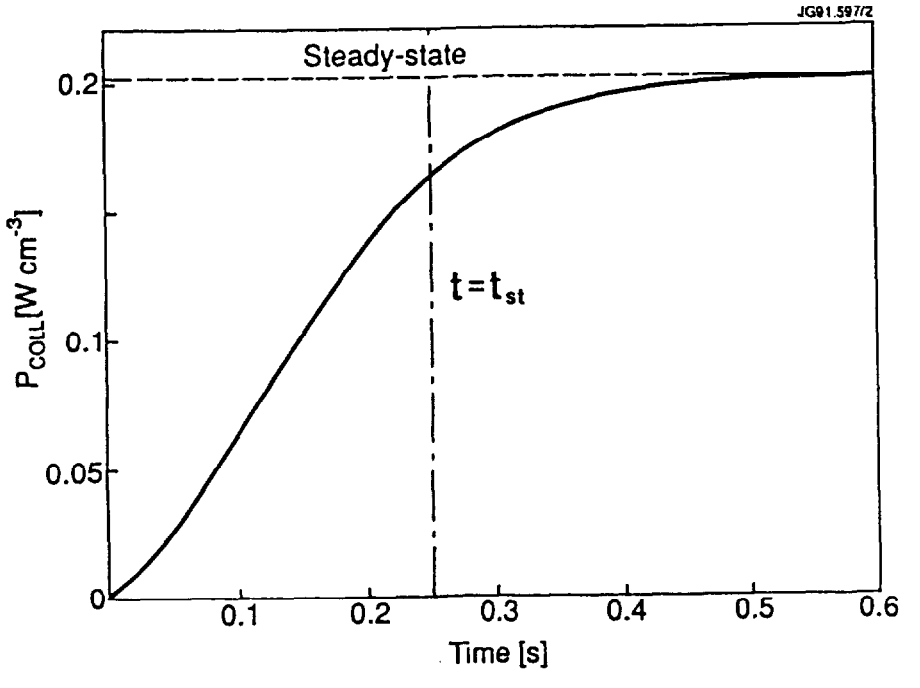

FIG. 2. — Collisional power transfer as a function of time for the test case data. The time it takes to establish the velocity distribution, t_{st}, is indicated.

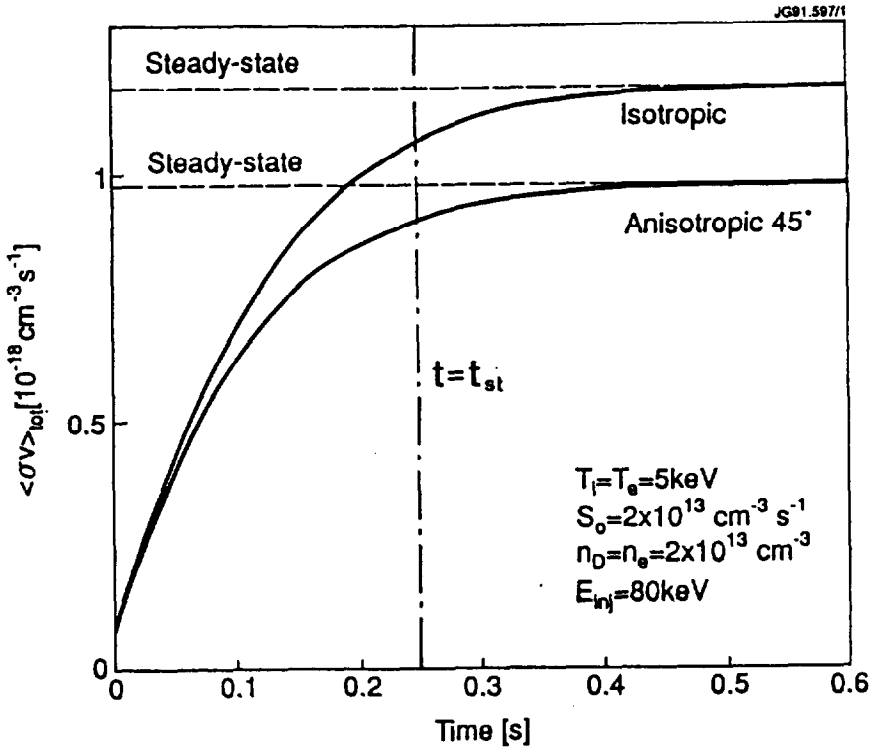

FIG. 3. — Evolution in time of the total fusion reactivities for DD neutrons for isotropic and anisotropic distributions.

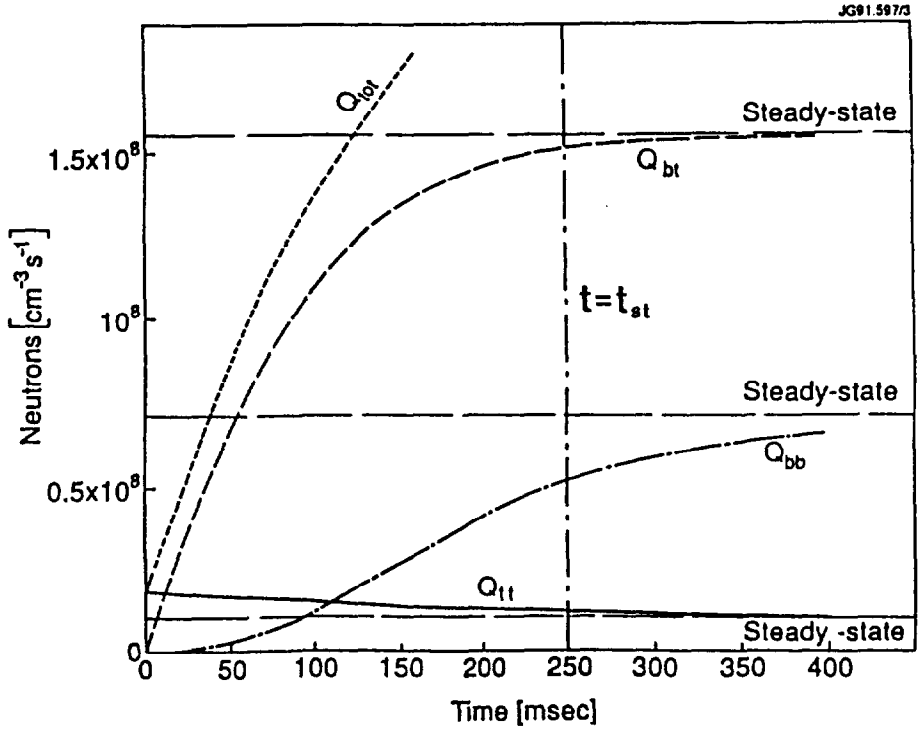

FIG. 4. — Thermal (Q_{tt}), beam-thermal (Q_{bt}) and beam-beam (Q_{bb}) neutron rates for the test case data as functions of time. The estimated time it takes to establish the velocity distribution below the injection energy, t_{st}, is indicated.

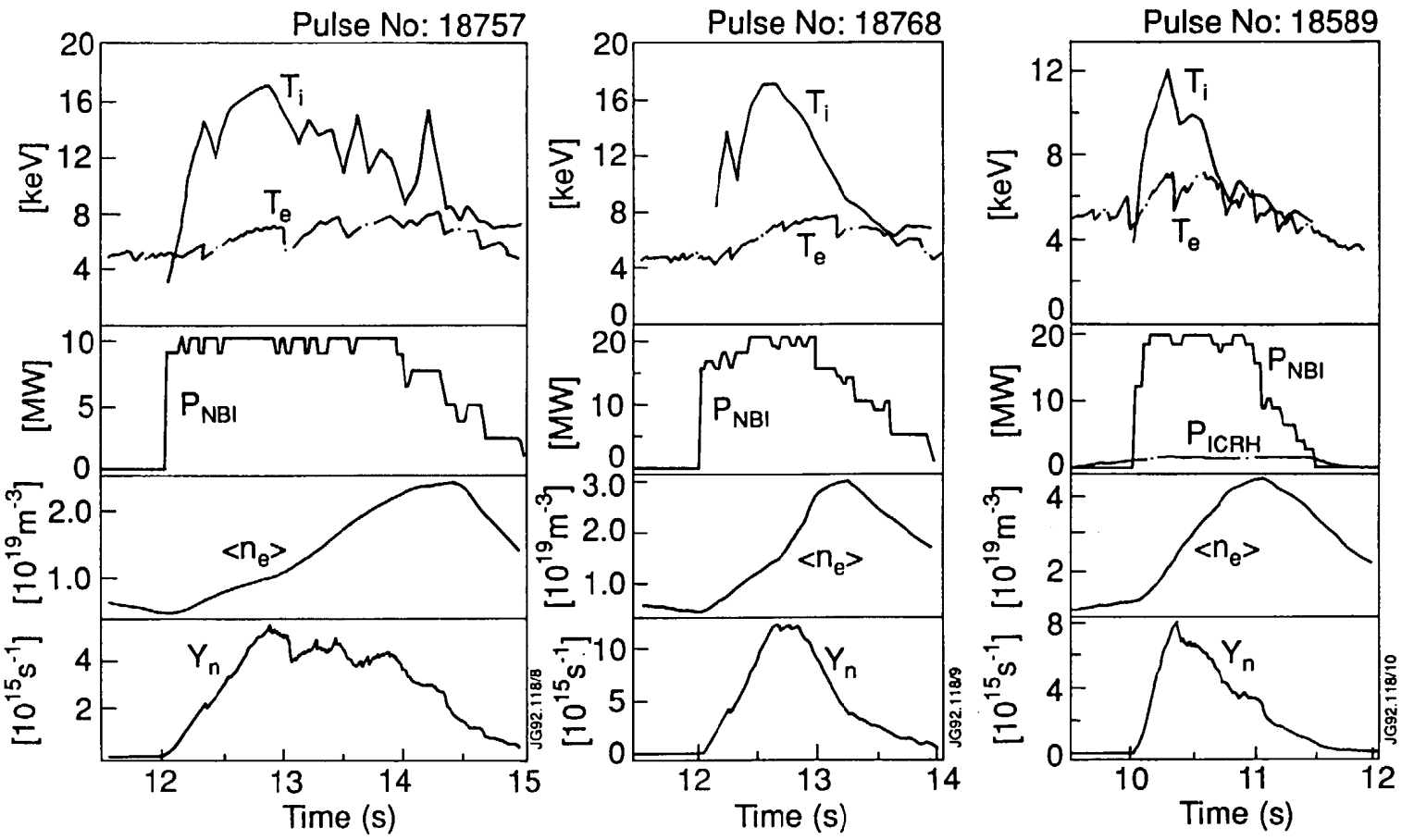

FIG. 5. – Time evolution of the main parameters in the discharges #18757, #18768 and #18589; T_i is the central ion temperature from the charge exchange recombination diagnostic, T_e is the central electron temperature from ECE, P_{NBI} is the total input beam power, P_{ICRH} is the total ICRH input power (#18589 only), $<n_e>$ is the volume average density and Y_n is the neutron yield.

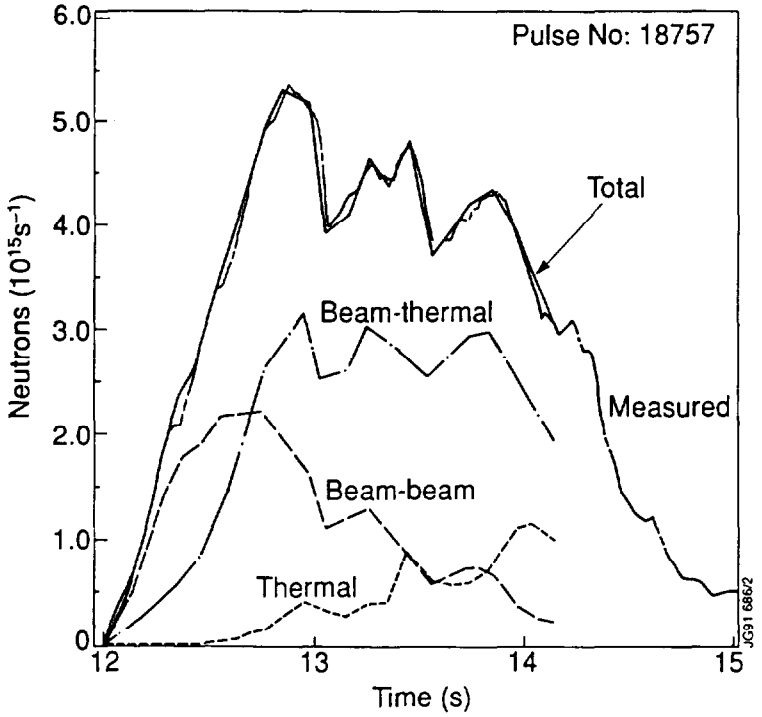

FIG. 6. – Measured and calculated neutron rates including the thermal, beam-thermal and beam-beam components versus time for pulse #18757.

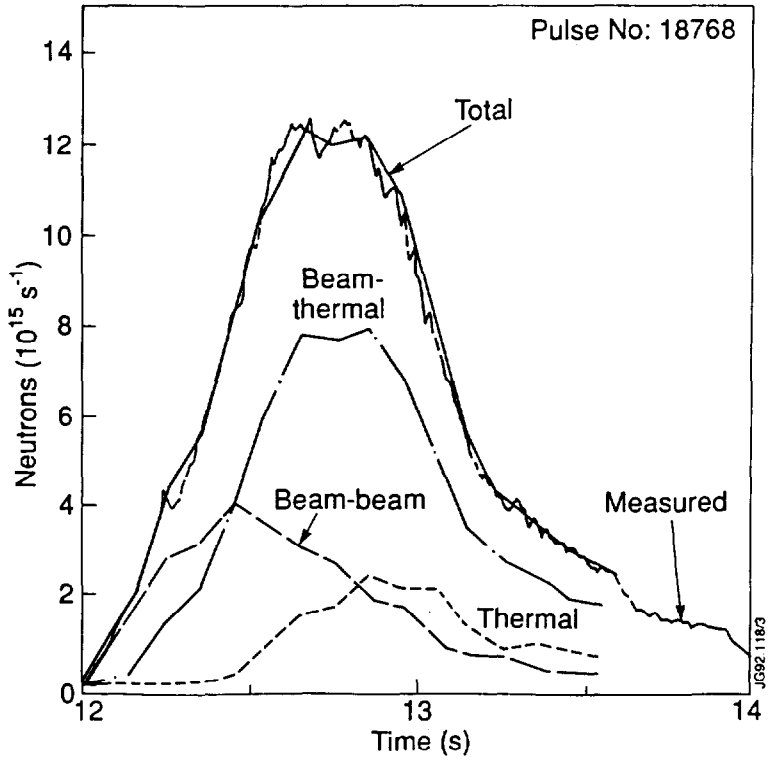

FIG. 7. – Calculated neutron emission and its composition due to thermal, beam-thermal and beam-beam emission together with the measured yield for discharge #18768.

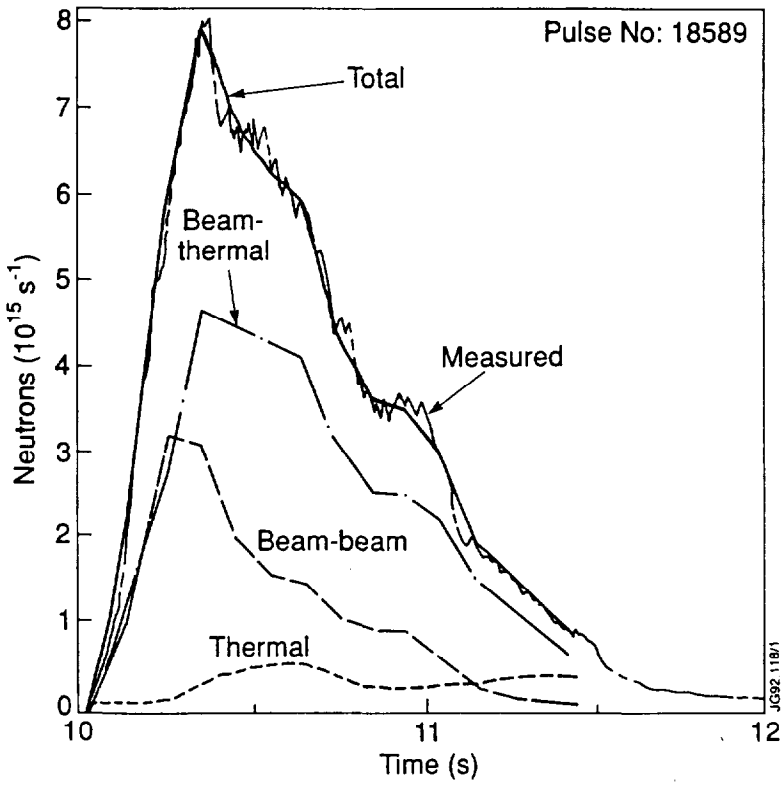

FIG. 8. — Time evolution of the measured and calculated neutron emission with the contribution from thermal, beam-thermal and beam-beam reactions for pulse #18589.

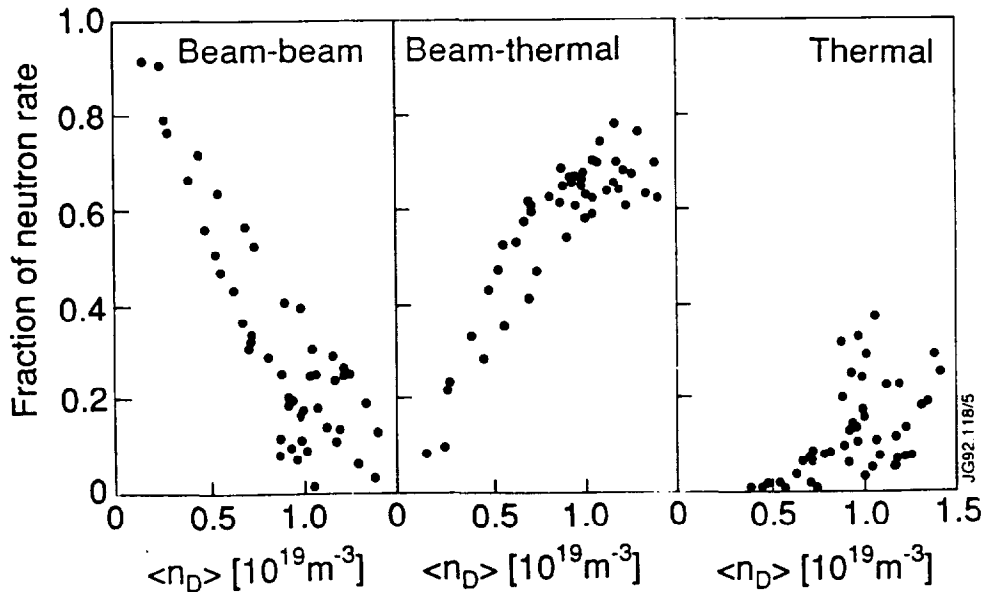

FIG. 9. — The composition of the neutron emission due to thermal, beam-thermal and beam-beam reactions at different time points for the pulses #18757, #18768 and #18589 versus the volume average deuteron density.

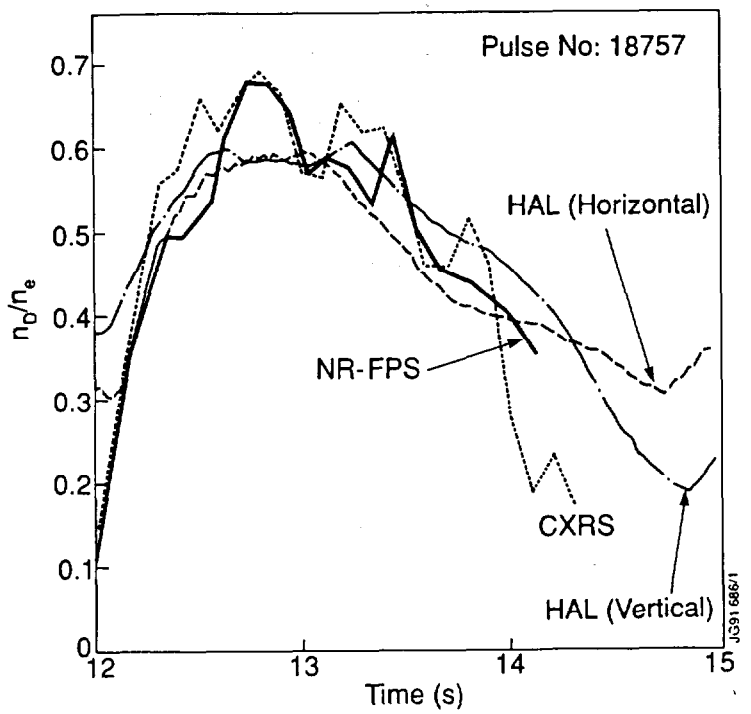

FIG. 10. — Calculated dilution ratio n_D/n_e as a function of time for pulse #18757 together with measured data from the charge exchange recombination diagnostic CXRS and visible bremsstrahlung Z_{eff} HAL.

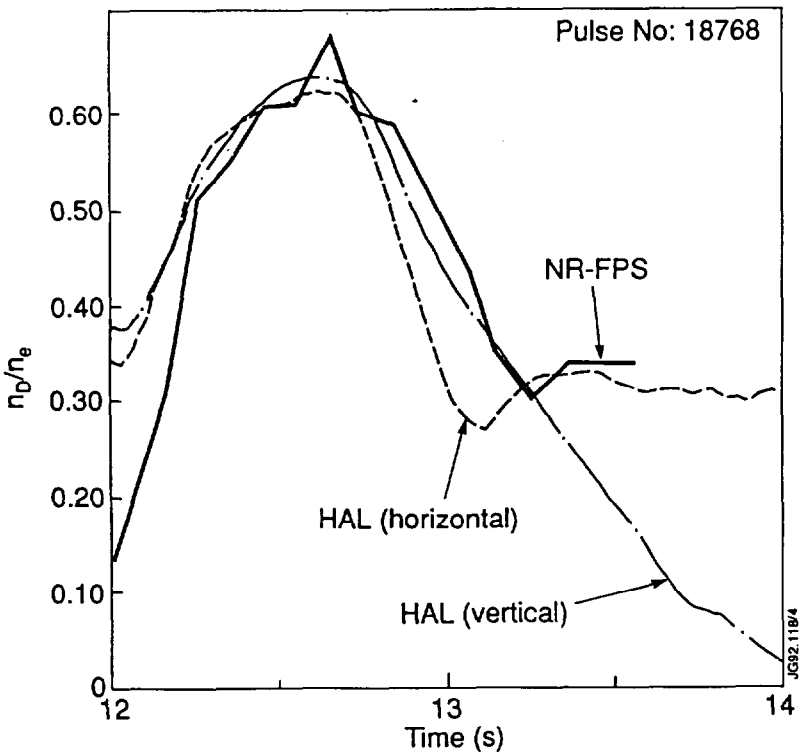

FIG. 11. — Calculated dilution ratio n_D/n_e as a function of time for pulse #18768 together with the dilution ratio derived from the visible bremsstrahlung Z_{eff} HAL.

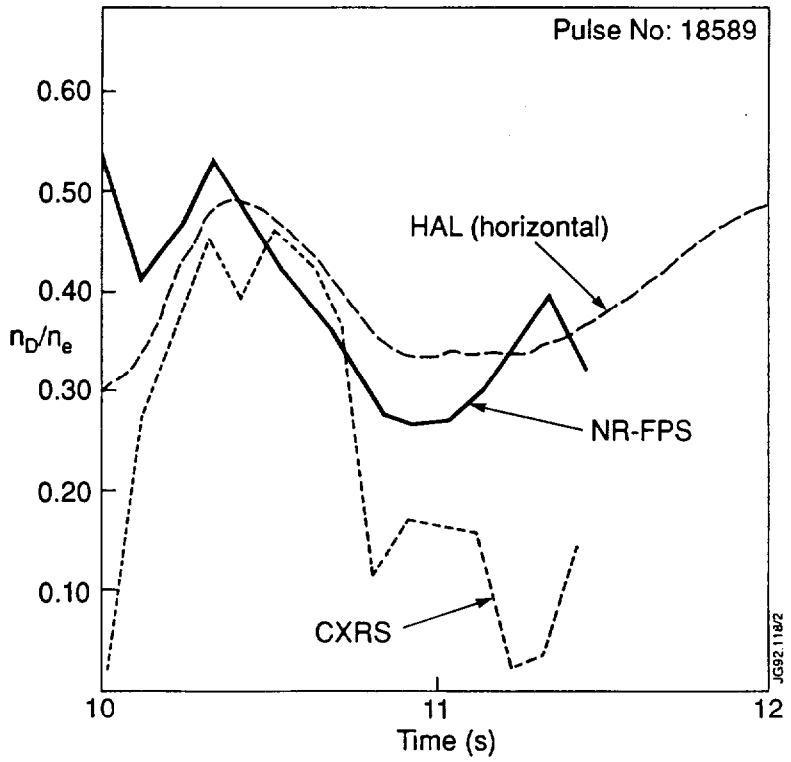

FIG. 12. – Calculated dilution ratio n_D/n_e as a function of time for pulse #18589 together with measured data from the CXRS diagnostic and dilution ratios derived from the visible bremsstrahlung Z_{eff} HAL.

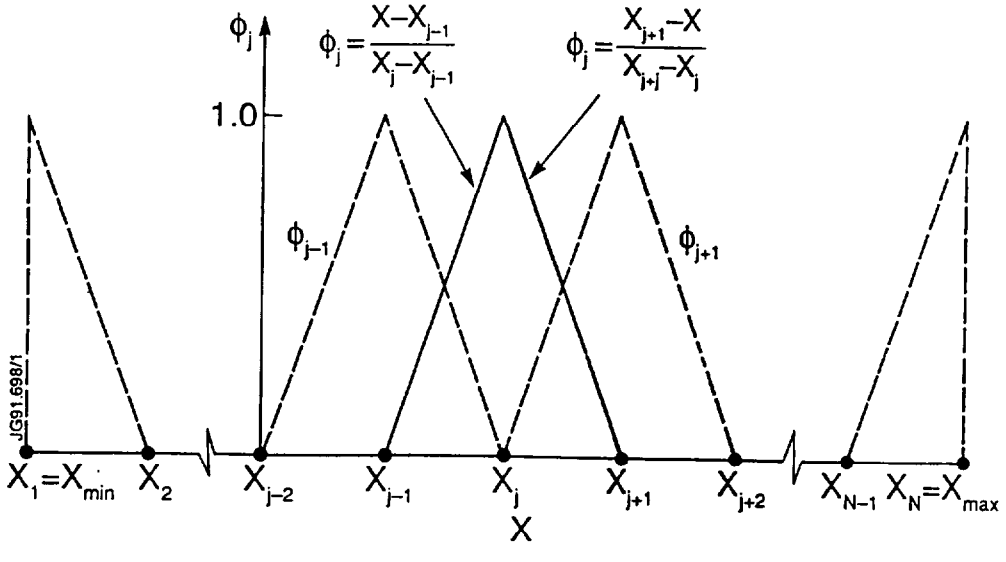

FIG. 13. – Linear finite elements.

STEP	CPU-TIME [%]
Set up	1.12
Calculate reactivity coefficients	0.59
Fokker-Planck solution	85.74
Output data calculation	12.55

TAB. 1. – Amount of CPU-time used by the code for analysing the discharge #18757.

ANNEX

P.-H. REBUT, A. GIBSON, M. HUGUET, J.M. ADAMS[1], B. ALPER, H. ALTMANN, A. ANDERSEN[2], P. ANDREW[3], M. ANGELONE[4], S. ALI-ARSHAD, P. BAIGGER, W. BAILEY, B. BALET, P. BARABASCHI, P. BARKER, R. BARNSLEY[5], M. BARONIAN, D.V. BARTLETT, L. BAYLOR[6], A.C. BELL, G. BENALI, P. BERTOLDI, E. BERTOLINI, V. BHATNAGAR, A.J. BICKLEY, D. BINDER, H. BINDSLEV[2], T. BONICELLI, S.J. BOOTH, G. BOSIA, M. BOTMAN, D. BOUCHER, P. BOUCQUEY, P. BREGER, H. BRELEN, H. BRINKSCHULTE, D. BROOKS, A. BROWN, T. BROWN, M. BRUSATI, S. BRYAN, J. BRZOZOWSKI[7], R. BUCHSE[22], T. BUDD, M. BURES, T. BUSINARO, P. BUTCHER, H. BUTTGEREIT, C. CALDWELL-NICHOLS, D.J. CAMPBELL, P. CARD, G. CELENTANO, C.D. CHALLIS, A.V. CHANKIN[8], A. CHERUBINI, D. CHIRON, J. CHRISTIANSEN, P. CHUILON, R. CLAESEN, S. CLEMENT, E. CLIPSHAM, J.P. COAD, I.H. COFFEY[9], A. COLTON, M. COMISKEY[10], S. CONROY, M. COOKE, D. COOPER, S. COOPER, J.G. CORDEY, W. CORE, G. CORRIGAN, S. CORTI, A.E. COSTLEY, G. COTTRELL, M. COX[11], P. CRIPWELL[12], O. Da COSTA, J. DAVIES, N. DAVIES, H. de BLANK, H. de ESCH, L. de KOCK, E. DEKSNIS, F. DELVART, G.B. DENNE-HINNOV, G. DESCHAMPS, W.J. DICKSON[13], K.J. DIETZ, S.L. DMITRENKO, M. DMITRIEVA[14], J. DOBBING, A. DOGLIO, N. DOLGETTA, S.E. DORLING. P.G. DOYLE, D.F. DÜCHS, H. DUQUENOY, A. EDWARDS, J. EHRENBERG, A. EKEDAHL, T. ELEVANT[7], S.K. ERENTS[11], L.G. ERIKSSON, H. FAJEMIROKUN[12], H. FALTER, J. FREILING[15], F. FREVILLE, C. FROGER, P. FROISSARD, K. FULLARD, M. GADEBERG, A. GALETSAS, T. GALLAGHER, D. GAMBIER, M. GARRIBBA, P. GAZE, R. GIANNELLA, R.D. GILL, A GIRARD, A. GONDHALEKAR, D. GOODALL[11], C. GORMEZANO, N.A. GOTTARDI, C. GOWERS, B.J. GREEN, B. GRIEVSON, R. HAANGE, A. HAIGH, C.J. HANCOCK, P.J. HARBOUR, T. HARTRAMPF, N.C. HAWKES[11], P. HAYNES[11], J.L. HEMMERICH, T. HENDER[11], J. HOEKZEMA, D. HOLLAND, M. HONE, L. HORTON, J. HOW, M. HUART, I. HUGHES, T.P. HUGHES[10], M. HUGON, Y. HUO[16], K. IDA[17], B. INGRAM, M. IRVING, J. JACQUINOT, H. JAECKEL, J.F. JAEGER, G. JANESCHITZ, Z. JANKOVICZ[18], O.N. JARVIS, F. JENSEN, E.M. JONES, H.D. JONES, L.P.D.F. JONES, S. JONES[19], T.T.C. JONES, J.-F. JUNGER, F. JUNIQUE, A. KAYE, B.E. KEEN, M. KEILHACKER, G.J. KELLY, W. KERNER, A. KHUDOLEEV[21], R. KONIG, A. KONSTANTELLOS, M. KOVANEN[20], G. KRAMER[15], P. KUPSCHUS, R. LÄSSER, J.R. LAST, B. LAUNDY, L. LAURO-TARONI, M. LAVEYRY, K. LAWSON[11], M. LENNHOLM, J. LINGERTAT[22], R.N. LITUNOVSKI, A. LOARTE, R. LOBEL, P. LOMAS, M. LOUGHLIN, C. LOWRY, J. LUPO, A.C. MAAS[15], J. MACHUZAK[19], B. MACKLIN, G. MADDISON[11], C.F. MAGGI[23], G. MAGYAR, W. MANDL[22], V. MARCHESE, G. MARCON, F. MARCUS, J. MART, D. MARTIN, E. MARTIN, R. MARTIN-SOLIS[24], P. MASSMANN, G. MATTHEWS, H. McBRYAN, G. McCRACKEN[11], J. McKIVITT, P. MERIGUET, P. MIELE, A. MILLER, J. MILLS, S.F. MILLS, P. MILLWARD, P. MILVERTON, E. MINARDI[4], R. MOHANTI[25], P.L. MONDINO, D. MONTGOMERY[26], A. MONTVAI[27], P. MORGAN, H. MORSI, D. MUIR, G. MURPHY, R. MYRNÄS[28], F. NAVE[29], G. NEWBERT, M. NEWMAN, P. NIELSEN, P. NOLL, W. OBERT, D. O'BRIEN, J. ORCHARD, J. O'ROURKE, R. OSTROM, M. OTTAVIANI, M. PAIN, F. PAOLETTI, S. PAPASTERGIOU, W. PARSONS, D. PASINI, D. PATEL, A. PEACOCK, N. PEACOCK[11], R.J.M. PEARCE, D. PEARSON[12], J.F. PENG[16], R. PEPE DE SILVA, G. PERINIC, C. PERRY, M. PETROV[21], M.A. PICK, J. PLANCOULAINE, J.-P POFFÉ, R. PÖHLCHEN, F. PORCELLI, L. PORTE[13], R. PRENTICE, S. PUPPIN, S. PUTVINSKII[8], G. RADFORD[30], T. RAIMONDI, M.C. RAMOS DE ANDRADE, R. REICHLE, J. REID, S. RICHARDS, E. RIGHI, F. RIMINI, D. ROBINSON[11], A. ROLFE, R.T. ROSS, L. ROSSI, R. RUSS, P. RUTTER, H.C. SACK, G. SADLER, G. SAIBENE, J.L. SALANAVE, G. SANAZZARO, A. SANTAGIUSTINA, R. SARTORI, C. SBORCHIA, P. SCHILD, M. SCHMID, G. SCHMIDT[31], B. SCHUNKE, S.M. SCOTT, L. SERIO, A SIBLEY, R. SIMONINI, A.C.C. SIPS, P. SMEULDERS, R. SMITH, R. STAGG, M. STAMP, P. STANGEBY[3], R. STANKIEWICZ[32], D.F. START, C.A. STEED, D. STORK, P.E. STOTT, P. STUBBERFIELD, D. SUMMERS, H. SUMMERS[13], L. SVENSSON, J.A. TAGLE[33], M. TALBOT, A. TANGA, A. TARONI, C. TERELLA, A TERRINGTON, A TESINI, P.R. THOMAS, E. THOMPSON, K. THOMSEN, F. TIBONE, A. TISCORNIA, P. TREVALION, B. TUBBING, P. VAN BELLE, H. VAN DER BEKEN, G. VLASES, M. VON HELLERMANN, T. WADE, C. WALKER, R. WALTON[31], D. WARD, M.L. WATKINS, N. WATKINS, M.J. WATSON, S. WEBER[34], J. WESSON, T.J. WIJNANDS, J. WILKS, D. WILSON, T. WINKEL, R. WOLF, D. WONG, C. WOODWARD, Y. WU[35], M. WYKES, D. YOUNG, I.D. YOUNG, L. ZANNELLI, A. ZOLFAGHARI[19], W. ZWINGMANN

[1] Harwell Laboratory, UKAEA, Harwell, Didcot, Oxfordshire, UK.
[2] Risø National Laboratory, Roskilde, Denmark.
[3] Institute for Aerospace Studies, University of Toronto, Downsview, Ontario, Canada.
[4] ENEA Frascati Energy Research Centre, Frascati, Rome, Italy.
[5] University of Leicester, Leicester, UK.
[6] Oak Ridge National Laboratory, Oak Ridge, TN, USA.
[7] Royal Institute of Technology, Stockholm, Sweden.
[8] I.V. Kurchatov Institute of Atomic Energy, Moscow, Russian Federation.
[9] Queens University, Belfast, UK.
[10] University of Essex, Colchester, UK.
[11] Culham Laboratory, UKAEA, Abingdon, Oxfordshire, UK.
[12] Imperial College of Science, Technology and Medicine, University of London, London, UK.
[13] University of Strathclyde, Glasgow, UK.
[14] Keldysh Institute of Applied Mathematics, Moscow, Russian Federation.
[15] FOM-Institute for Plasma Physics "Rijnhuizen", Nieuwegein, Netherlands.
[16] Institute of Plasma Physics, Academia Sinica, Hefei, Anhui Province, China.
[17] National Institute for Fusion Science, Nagoya, Japan.
[18] Soltan Institute for Nuclear Studies, Otwock/Świerk, Poland.
[19] Plasma Fusion Center, Massachusetts Institute of Technology, Boston, MA, USA.
[20] Nuclear Engineering Laboratory, Lappeenranta University, Finland.
[21] A.F. Ioffe Physico-Technical Institute, St. Petersburg, Russian Federation.
[22] Max-Planck-Institut für Plasmaphysik, Garching, Germany.
[23] Department of Physics, University of Milan, Milan, Italy.
[24] Universidad Complutense de Madrid, Madrid, Spain.
[25] North Carolina State University, Raleigh, NC, USA.
[26] Dartmouth College, Hanover, NH, USA.
[27] Central Research Institute for Physics, Budapest, Hungary.
[28] University of Lund, Lund, Sweden.
[29] Laboratorio Nacional de Engenharia e Tecnologia Industrial, Sacavem, Portugal.
[30] Institute of Mathematics, University of Oxford, Oxford, UK.
[31] Princeton Plasma Physics Laboratory, Princeton University, Princeton, NJ, USA.
[32] RCC Cyfronet, Otwock/Świerk, Poland,
[33] Centro de Investigaciones Energéticas, Medioambientales y Tecnológicas, Madrid, Spain.
[34] Freie Universität, Berlin, Germany.
[35] Insitute for Mechanics, Academia Sinica, Beijing, China.